Science and Technology

RMUTT Journal

Vol.10 No.1 (2020) : 237-244

www.sci.rmutt.ac.th/stj

Online ISSN 2229-1547

Oxidative Addition of bromobenzene on Au_{20} and $Au_{10}Pd_{10}$: Evidenced by Density Functional Theory Calculations

Sirichai Sooksathit[1], Aurucha Kittisabhorn[1], Jutaporn Treesing[1], Preecha Mansalai[1], Singto Sakulkhaemaruethai[1], Somchai Uapipatanakul[2], Boontida Uapipatanakul[1*] and Karan Bobuatong[1*]

[1]Department of Chemistry, Faculty of Science and Technology, Rajamagala University of Technology Thanyaburi, Pathum Thani 12110, Thailand

[2]Kinetics Corporation Ltd, 388 Ratchadapisek Rd. 32, Chadrakasem, Chatuchak Bangkok 10900, Thailand

*E-mail: karan_b@rmutt.ac.th

Abstract

The unusual catalytic activity of bimetallic Au/Pd alloy nanocluster for Ullmann coupling reaction of bromobenzene has been theoretically investigated by mean of DFT with M06 functional. It is found that two factors governing the catalytic activity of Au/ Pd towards bromobenzene are the stability of dissociative chemisorption in the oxidative addition step and leaching of Pd during the progress of the reaction. The differences in catalytic activity between bimetallic Au/Pd and monometallic Au are also discussed.

Keywords: Oxidative Addition, bromobenzene, bimetallic Au/Pd, DFT

1. Introduction

The synthetic methods of symmetrical biaryls have been the subject of considerable attention since the discovery of the Ullmann coupling reaction in the early 19th century [1]. The traditional Ullmann coupling reaction is the copper-mediated nucleophilic aromatic substitution of aromatic halides which is, however, required stoichiometric amounts of copper salts together with high reaction temperatures (≥ 200°C) and long reaction time. Several reviews on this reaction and subsequent developments of alternative copper-

Received: June 04, 2020

Revised: June 19, 2020

Accepted: June 21, 2020

based methodologies have discussed in great detail [2], [5]. Despite, Dhital *et al*. have introduced a new strategy to overcome these limitations by using the bimetallic gold/ palladium alloy stabilized by poly(N-vinyl-2-pyrrolidone) (PVP) as the catalyst (Figure 1a) [6]. The use of such catalyst enables us to perform Ullmann coupling of chloroarenes under low temperature (27-35°C) providing a certain high selectivity and yield to the desired products. Moreover, the bimetallic nanocluster was found to have higher catalytic activity toward chloroarenes than their Bromo equivalents and completely inhibit the coupling of aryl iodides [7]. This surprising finding is in the opposite trend with the conventional reactivity of aromatic halides in the oxidative addition processes, the first elementary step of Ullmann coupling reaction (aryl iodides>aryl bromides> aryl chlorides). Up to the present time, the origin of different catalytic activity of such reaction is not clearly understood and remains considerable debate. Therefore, in this work, we have performed theoretically mechanistic investigation to address the fundamental questions regarding the unusual activity of the Ullmann coupling reaction catalyzed by bimetallic gold/palladium alloy.

As a part of our efforts to investigate the reaction mechanisms occurred on Au and AuPd nanoclusters (NCs), we have successfully employed DFT with M06 functional to

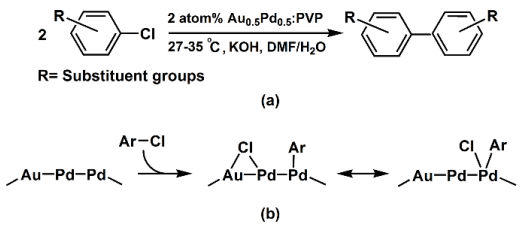

Figure 1 (a) Ullmann coupling of chloroarenes catalyzed by Au/Pd:PVP catalyst (b) Oxidative addition of chloroarenes on Au/Pd surface.

estimate the stability of intermediates and transition structures as well as activation barriers of interest [6]. We found that, an essential step, which determines the characteristics difference in the catalytic activity of Au and AuPd NCs of Ullmann coupling of chloroarene is the oxidative addition resulting in C−Cl bond dissociation followed by the spillover of Cl atom (Figure 1b). The high catalytic activity of the AuPd NCs is due to the substrate being adsorbed effectively onto the alloy surface and the subsequent activation barriers of oxidative addition are significantly small, which is unlikely to occur with single metal gold catalysts.

2. Model and Method

To investigate the reaction mechanism of oxidative addition on the Au and Au/ Pd alloy nanoclusters (NC) stabilized by poly(N-vinyl-2-pyrrolidone) (PVP), we select 20-atom gold and gold/ palladium NCs, Au_{20} and $Au_{10}Pd_{10}$, as the model system because we have recently shown that Au_{20} and $Au_{10}Pd_{10}$ are the practical catalyst models

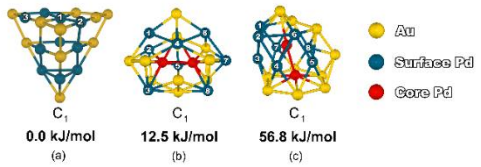

Figure 2 $Au_{10}Pd_{10}$ structures with point group symmetries and the corresponding relative energies (kJ/mol) for (a) DFT-fit (b) exp-fit (c) average.

for the theoretical study of the oxidation reactions on Au and Au/Pd alloy NCs [6], [7]. Global optimization of Au/Pd NCs were performed using a genetic algorithm, coupled with the Gupta many-body empirical potential. Three sets of Gupta potential parameters have been employed in this work: (a) an average of pure Pd and Au parameters, (b) experimental Pd-Au-fitted parameters, and (c) DFT-fitted parameters, as listed in Ref12.

Subsequently, we performed structural optimization for $Au_{10}Pd_{10}$ NCs obtained after global minima searching by DFT calculation with M06 functional which has recently been proven useful for the study of physical and chemical properties of gold such as its dimensionality and the chemical reactions catalyzed by gold NCs [10], [11]. All calculations in this part were carried out using the GAUSSIAN 09 suite of programs [12]. The full electron calculation is rather time-consuming; therefore, it is better to introduce effective core potentials including relativistic effects (RECP) for the Au (Xe core) and Pd (Kr core) atoms in order to describe the inner core electrons. Under this approximation, the 19 valence electrons in the outer shell (5s5p5d6s) of the Au atom and the 18 valence electrons in the outer shell (4s4p4d) of the Pd atom are described through the corresponding LanL2DZ basis sets [18]. The 6-31G(d,p) basis sets were employed for hydrogen and carbon atoms. During the optimization, all catalyst clusters and substrates were fully relaxed without any symmetry constraints. The default convergence thresholds of the maximum force, root-mean-square (RMS) force, the maximum displacement of atoms, and RMS displacement were set to 0.00045, 0.0003, 0.0018, and 0.0012 a.u., respectively. The free energies of Pd-Leaching on Au, AuPd and Pd NCs were calculated in the presence of a continuum solvation approach, SMD [19]. Six components of d-functions and ten components of f-functions were also employed to examine Pd-Leaching process. All the ground state optimized structures are local minima; vibrational analysis performed at the optimized structures contained no imaginary frequencies. The Synchronous Transit-Guided Quasi-Newton (STQN) Method, developed by H. B. Schlegel and coworkers was employed in order to approach the quadratic region around the transition states [20]. All the optimized transition state structures possessed only one imaginary frequency in the range of -1,500-1,200 cm^{-1} indicating the true transition state connected to the corresponding the local minima structures.

3. Results and Discussion

3.1 Model of Gold-Palladium clusters

In comparison between optimized $Au_{10}Pd_{10}$ NCs, we found that the stability of

$Au_{10}Pd_{10}$ NCs is in order of DFT- fit>exp-fit>average. Nevertheless, one can see that there is not much difference in the relative energy between the DFT-fit and exp-fit configuration (Figure 2). Therefore, we chose these two $Au_{10}Pd_{10}$ NCs to examine further examine the oxidative addition of bromobenzene in the next step. In addition, it is of interest to compare the catalytic activity between bimetallic AuPd NC and monometallic Au NC. Therefore, we also used Au_{20}, which have been demonstrated as a suitable model for simulating the reactions on the surface of Au: PVP [6,15] as a catalyst model and then compared the calculated results between them

Regarding the optimized $Au_{10}Pd_{10}$ NCs, it appears that there are three and eight surface Pd atoms located in different environment of DFT-fit and exp- fit, respectively. We performed the calculations of the oxidative addition of bromobenzene on all these Pd atoms and found that such reaction is energetically preferred to take place on Pd1 of DFT-fit (Figure 2) due to the lowest activation barrier of 29.5 kJ/mol (see Table 1). Next, we compare the calculated results with mono metallic Au NC as follows.

3.2 Reaction mechanism

In this study, we have proposed the oxidative addition of bromobenzene which takes place on Au_{20} and $Au_{10}Pd_{10}$ in the same manner as our recent previous study (Figure 3). The reaction is initiated by the adsorption of bromobenzene forming π-complex interaction between π bond of bromobenzene and metal atoms on the facet site of Au_{20} and on the Pd1 of $Au_{10}Pd_{10}$ (exp-fit) NCs, respectively. It appears that the ligand (electronic) effect plays an important role for this step of the reaction. The structures of bromobenzene adsorbed on $Au_{10}Pd_{10}$ is significantly changed compared with that of Au_{20} mainly because of the stronger interaction (-131.3 vs. -178.4 kJ/mol). The average C– C bond distances of bromobenzene are lengthened from 1.391 Å (isolated species) to 1.392 Å and 1.423 Å for the adsorption on Au_{20} and $Au_{10}Pd_{10}$, respectively.

Considering the transition states of C – Br dissociation, we found that the role of Pd is not only to enhance the stability of the adsorption complex on $Au_{10}Pd_{10}$, but also significantly stabilize the

Table 1. Calculated energies of adsorption complexes (Ads), transition states (TS), intermediates and activation barriers (Ea) involved the oxidative addition of bromobenzene on $Au_{10}Pd_{10}$ with DTF-fit and exp-fit configurations (kJ/mol).

	Ads	TS	Int	E_a
DFT-fit				
Pd1	-160.4	-113.3	-234.9	47.1
Pd2	-167.4	-108.1	-241.7	59.3
Pd3	-176.4	-105.1	-241.7	71.3
exp-fit				
Pd1	-178.4	-148.9	-255.5	29.5
Pd2	-122.1	-84.0	-211.8	38.1
Pd3	-151.7	-112.8	-195.4	38.9
Pd4	-155.8	-120.4	-188.3	35.4
Pd5	-135.5	-89.6	-212.0	45.9
Pd6	-174.7	-127.0	-247.6	47.7
Pd7	-174.7	-138.9	-262.1	35.8
Pd8	-163.0	-112.9	-184.9	50.1

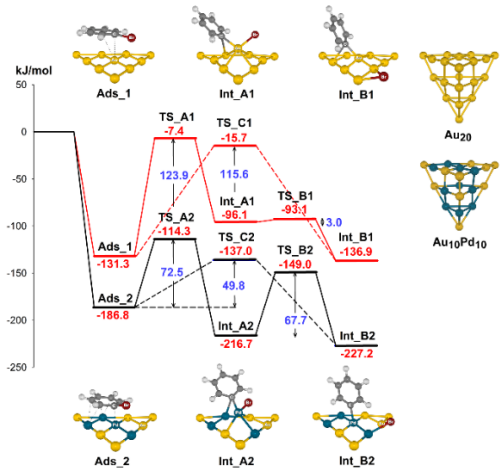

Figure 3 Energy profile diagram of oxidative addition of bromobenzene on Au_{20} and $Au_{10}Pd_{10}$ NCs.

corresponding transition structures. As shown in Figure 3, it is clearly shown that in the presence of Pd atom on the surface of $Au_{10}Pd_{10}$ NC, the transition states of C−Br bond dissociation (TS_A2 and TS_C2) are significantly more stable than those of Au_{20} (TS_A1 and TS_C1) yielding as a consequence the lower activation barriers (123.9 vs 72.5 kJ/mol). The high activation barriers of C−Br bond dissociation on Au_{20} could support the experimental results that the reaction does not take place with gold single-metal nanocluster alone, nor with a physical mixture of the gold and palladium metals [6].

Furthermore, our results indicate that these bond dissociations are energetically preferred via the transition states associated with the formation of adsorbed phenyl group on Pd atom and adsorbed Br on the next-nearest-neighbor Au−Pd (Int_B2) due to the low activation barrier of 49.8 kJ/ mol. Nevertheless, an alternative reaction pathway that directly provides phenyl group and Br attached on the same Pd atom (Int_A2), is also responsible for this reaction. We found that adsorbed Br can undergo the spillover on the surface of $Au_{10}Pd_{10}$ requiring activation energies of 66.7 kJ/mol.

It is worthy of note that even the activation barriers of C− Br dissociation are comparable with the conventional trend for the reactivity of aromatic halides in oxidative addition processes (bromides>chlorides), the calculated adsorption energies of intermediates on $Au_{10}Pd_{10}$ exceed - 200 kJ/ mol indicating the very strong interaction of such intermediates on $Au_{10}Pd_{10}$. These interactions are probably too strong to proceed with the rest of coupling reaction proposed in our previous study including oxidation addition of another benzyl halides and subsequent reductive elimination. At this point, we suggest that such strong interactions might be an explanation for the unusual catalytic activity of $Au_{0.5}Pd_{0.5}$:PVP in which the Ullmann coupling reaction of bromobenzene is slower than that of chlorobenzene and it shows no catalytic activity towards Iodobenzene [7]. In this article, we also investigate the possibility of the leaching process of surface Pd from $Au_{10}Pd_{10}$ NC if oxidative addition occurs on a single metal atom to afford Pd(II) intermediate (equation 1 and Figure 4). The free energies (ΔG_{298}) of such process, which were calculated using a new continuum solvation model developed by Truhlar and co-workers [19], are listed in Table 2.

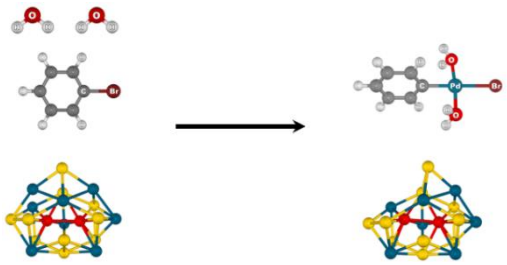

Figure 4 Pd-leaching during the oxidative addition of bromobenzene on $Au_{10}Pd_{10}$ cluster in the presence of waters.

$$C_6H_5Br+2H_2O+Au_{10}Pd_{10} \rightarrow C_6H_5Pd(H_2O)_2Br+Au_{10}Pd_9 \quad (1)$$

Based on our results, it indicates that the leaching of surface Pd atoms from $Au_{10}Pd_{10}$ cluster could take part in the catalytic cycle. In other word, we suggest that catalysis in the oxidative addition of bromobenzene might occur involving atomic Pd leached from $Au_{10}Pd_{10}$ to afford $Au_{10}Pd_9$ and $C_6H_5Pd(H_2O)_2Br$. Since the Ullmann coupling reaction was identified to occur on the surface of $Au_{0.5}Pd_{0.5}$:PVP, the leaching of Pd could be a factor that determines the relative low catalytic activity of $Au_{10}Pd_{10}$ towards aryl bromides in comparison with aryl chlorides.

Table 2. Calculated free energies of leaching process of Pd from $Au_{10}Pd_{10}$ (ΔG_{298}).

Catalyst models	ΔG_{298} (kJ/mol)
DFT-fit	
Pd1	-18.5
Pd2	-16.0
Pd3	-17.5
exp-fit	
Pd1	-39.5
Pd2	-24.8
Pd3	-15.5
Pd4	-12.5
Pd5	-0.2
Pd6	-8.4
Pd7	-13.7
Pd8	-33.4

4. Conclusions

In summary, we have theoretically demonstrated that $Au_{10}Pd_{10}$ shows the same trend in the reactivity of aromatic halides for oxidative addition processes (bromide>chloride) because it requires small activation energies. However, the catalytic activity of $Au_{10}Pd_{10}$ for the first step of the Ullmann coupling reaction of bromobenzene could be suppressed by two factors including the relatively high stability of dissociative chemisorption and leaching of Pd during the progress of the reaction. The oxidative addition of bromobenzene cannot take place on the monometallic gold cluster (Au_{20}) due to the high activation barriers of C−Br bond activation which is in agreement with experimental observation.

5. Acknowledgments

Sirichai Sooksathit would like to acknowledge the support by Research and Researchers for Industries (RRI), Project No. MSD60I0096. The support from Institute of Research and Development, RMUTT, Thailand (Project No. DRF04066204) is also acknowledged. Karan Bobuatong thanks the support by The Thailand research Fund (TRF) (Project No. MRG5980142). The computations were partially performed in HPC, National e- Science Infrastructure Consortium, NECTEC, NSTDA, Thailand.

6. References

[1] Ullmann F. and Bielecki J. Ueber Synthesen in der Biphenylreihe. *Chem. Ber.* 1901. 34: 2174-2185. b) Ullmann F. Catalytic CC, CN, and CO Ullmann-Type Coupling Reactions: Copper Makes a Difference. *Ber. Dtsch. Chem. Ges.* 1903. 36: 2382-2384. c) Goldberg I. Ueber Phenylirungen bei Gegenwart von Kupfer als Katalysator. *Ber. Dtsch. Chem. Ges*. 1906. 39: 1691-1692.

[2] Hassan J., Sevignon M., Gozzi C., E. and Lemaire M. Aryl-Aryl Bond Formation One Century after the Discovery of the Ullmann Reaction. *Chem. Rev*. 2002. 102: 1359–1470.

[3] Sainsbury M. Modern methods of aryl-aryl bond formation. *Tetrahedron* 1980. 36: 3327-3359.

[4] Bringmann G., Walter R. and Weirich R. Der gezielte Aufbau von Biarylverbindungen: Moderne Konzepte and Strategien. *Angew. Chem*. 1990. 102: 1006-1019.

[5] Sperotto E., G. P. van Klink M., van Koten G. and de Vries J. G. The mechanism of the modified Ullmann reaction. *Dalton Trans*. 2010. 39: 10338-10351.

[6] Dhital R. N., Kamonsatikul C., Somsook E., Bobuatong K., Ehara M., Karanjit S. and Sakurai H. Low-Temperature Carbon–Chlorine Bond Activation by Bimetallic Gold/ Palladium Alloy Nanoclusters: An Application to Ullmann Coupling. *J. Am. Chem. Soc*. 2012. 134: 20250-20253.

[7] Dhital R. N., Kamonsatikul C., Somsook E., Sato Y. and Sakurai H. Aryl iodides as strong inhibitors in gold and gold-based bimetallic quasi-homogeneous catalysis. Chem. Commun. 2013. 49: 2542-2544.

[8] Cleri F. and Rosato V. Tight-binding potentials for transition metals and alloys. *Phys, Rev. B* 1993. 48: 22.

[9] Johnston R. L. Evolving better nanoparticles: Genetic algorithms for optimising cluster geometries. *Dalton Trans*. 2003. 4193-4207.

[10] Pittaway F., Paz-Borbo´n L. O., Johnston R. L., Arslan H., Ferrando R., Mottet C., Barcaro G. and Fortunelli A. Theoretical Studies of Palladium-Gold Nanoclusters: Pd-Au Clusters with up to 50 Atoms. J. Phys. Chem. C. 2009. 113: 9141-9152.

[11] Zhao Y. and Truhlar D. The M06 suite of density functionals for main group thermochemistry, thermochemical kinetics, noncovalent interactions, excited states, and transition elements: two new functionals and systematic testing of four M06-class functionals and 12 other functionals. *Theor. Chem. Acc*. 2008. 120: 215-241.

[12] Gaussian 09, Revision B.01, Frisch M. J., Trucks G. W., Schlegel H. B., Scuseria G. E., Robb M. A., Cheeseman J. R., Scalmani G., Barone V., Mennucci B., Petersson G. A., Nakatsuji H., Caricato M., Li X., Hratchian H. P., Izmaylov A. F., Bloino J.,

Zheng G., Sonnenberg J. L., Hada M., Ehara M., Toyota K., Fukuda R., Hasegawa J., Ishida M., Nakajima T., Honda Y., Kitao O., Nakai H., Vreven T., Montgomery J. A. Jr., Peralta J. E., Ogliaro F., Bearpark M., Heyd J. J., Brothers E., Kudin K. N., Staroverov V. N., Kobayashi R., Normand J., Raghavachari K., Rendell A., Burant J. C., Iyengar S. S., Tomasi J., Cossi M., Rega N., Millam J. M., Klene M., Knox J. E., Cross J. B., Bakken V., Adamo C., Jaramillo J., Gomperts R., Stratmann R. E., Yazyev O., Austin A. J., Cammi R., Pomelli C., Ochterski J. W., Martin R. L., Morokuma K., Zakrzewski V. G., Voth G. A., Salvador P., Dannenberg J. J., Dapprich S., Daniels A. D., Farkas Ö., Foresman J. B., Ortiz J. V., Cioslowski J. and Fox D. J. Gaussian, Inc., Wallingford CT, 2010.

[13] Mejía-Rosales S. J., Fernández-Navarro C., Pérez-Tijerina C. E., Blom D. A., Allard L. F. and José-Yacamán M. On the Structure of Au/Pd Bimetallic Nanoparticles. *J. Phys. Chem. C*. 2007. 111: 1256-1260.

[14] Luo K., Wei T., Yi C. W., Axnanda S. and Goodman D. W. J. Preparation and Characterization of Silica Supported Au—Pd Model Catalysts. *J. Phys. Chem. B*. 2005. 109: 23517-23522.

[15] Bobuatong K., Karanjit S., Fukuda R., Ehara M. and Sakurai H. Aerobic oxidation of methanol to formic acid on Au_{20}^-: a theoretical study on the reaction mechanism. *Phys. Chem. Chem. Phys*. 2012. 14: 3103-3111.

[16] Marenich A. V., Cramer C. J. and Truhlar D. G. Universal Solvation Model Based on Solute Electron Density and on a Continuum Model of the Solvent Defined by the Bulk Dielectric Constant and Atomic Surface Tensions. *J. Phys. Chem. B*. 2009. 113: 6378-6396.

[17] Dhital R. N. and Sakurai H. Anomalous Efficacy of Bimetallic Au/Pd Nanoclusters in C–Cl Bond Activation and Formal Metathesis-type C–B Bond Activation at Room Temperature. *Chem. Lett*. 2012. 41: 630-632.

[18] Feller D. The role of databases in support of computational chemistry calculations. *J. Comp. Chem*. 1996. 17: 1571-1586.

[19] Marenich A. V., Cramer C. J., and Truhlar D. G., Universal Solvation Model Based on Solute Electron Density and on a Continuum Model of the Solvent Defined by the Bulk Dielectric Constant and Atomic Surface Tensions. *J. Phys. Chem. B* 2009. 113: 6378-6396.

[20] Peng C., and Schlegel H. B., Combining Synchronous Transit and Quasi-Newton Methods for Finding Transition States. *Israel J. Chem*., 33 1993. 449-54.